Insight into the Short-Range Structure of Amorphous Iron Inositol Hexaphosphate as Provided by 31 P NMR and Fe X-ray Absorption Spectroscopy

ARTICLE *in* THE JOURNAL OF PHYSICAL CHEMISTRY B · DECEMBER 2006

Impact Factor: 3.3 · DOI: 10.1021/jp0633805 · Source: PubMed

An insight into the short-range structure of amorphous iron inositol hexaphosphate as provided by ^{31}P NMR and Fe X-ray absorption spectroscopy

Gregor Mali[a*], *Martin Šala*[b], *Iztok Arčon*[c,d], *Venčeslav Kaučič*[a] *and Jana Kolar*[b]

[a] National Institute of Chemistry, Hajdrihova 19, SI-1001 Ljubljana, Slovenia, [b] University of Ljubljana, Faculty of Chemistry and Chemical Technology, Aškerčeva 5, SI-1000 Ljubljana, Slovenia, [c] University of Nova Gorica, Vipavska 13, SI-5000 Nova Gorica, Slovenia, [d] Jožef Stefan Institute, Jamova 39, SI-1000 Ljubljana, Slovenia

RECEIVED DATE

^{31}P NMR and Fe EXAFS of iron phytates

Corresponding author's e-mail address: gregor.mali@ki.si

Short-range structure and formation of amorphous aggregates of iron inositol hexaphosphate (iron phytate) were studied by broadline solid-state ^{31}P NMR and Fe X-ray absorption spectroscopy. It was shown that bonds P-O-Fe with strong covalent character exist in solid substances. Iron in these substances is octahedrally coordinated by six oxygen atoms and further monodentatly bonded to three or four phosphorus atoms. In this way iron generates -P-O-Fe-O-P- intermolecular connections. An insight into formation of the network was obtained by studying structural changes in iron phytates with increasing concentration of iron. It was shown that the solid network builds when at least four out of six phosphate groups per one phytic molecule bond to iron atoms and thus participate in the intermolecular connections. This leads to iron phytate with approximately two iron atoms per one molecule of phytate. When concentration of iron in aggregates increases, the number of P-O-Fe bonds, and thus the number of phosphate groups that are bonded to iron, increases. Solid iron phytate with approximately four iron atoms per one molecule of phytate is almost saturated with iron. Its short-range structural properties can be explained well by a structure that is approaching an idealized model, in which each phosphate group is bonded to two iron atoms, and each iron atom is bonded to three phosphorus atoms and is shared between two phytic molecules.

Keywords iron, *myo*-inositol hexaphosphate, phytate, solid-state structure, NMR, EXAFS

Introduction

myo-Inositol hexaphosphoric acid (phytic acid, Scheme 1) is a ubiquitous and important molecule found in most cereals, nuts, legumes and oil-seeds. It possesses tremendous potential for chelating metal ions. Phytic acid and iron(III) are thought to form insoluble complexes which are not available for absorption under the pH conditions of the small intestine.[1] Thus induced negative effects on the bioavailability of iron and other essential minerals were described in several studies.[1,2] On the other hand, many investigations show that by forming an iron chelate, phytic acid suppresses iron-catalyzed oxidative reactions and serves not only as an antioxidant in the preservation of seeds but also as one of the most promising cancer chemopreventive agents.[3] The interaction between phytic acid and ferric ions is also important in the field of cultural heritage preservation. The two color-forming ingredients in one of the most widespread inks in the history of the western world, iron gall ink, were gallic acid from the tannins and iron ions. Unfortunately, these two components have induced severe degradation or even a complete destruction of numerous historical artefacts. It was shown relatively recently that treatment of documents with phytic acid may help to preserve them.[4-6]

The above described properties and potential applications of phytic acid raised our interest in the complexes formed between iron(III) ions and this acid. Several papers are describing conformational studies and complexation of phytate in solutions with different metal ions.[7,8] In case of iron, addition of 0.2 moles of ferric ions to one mole of phytic acid already results in aggregation and precipitation. Because the resulting solid substance is amorphous, its structure cannot be obtained by diffraction techniques. In this contribution, therefore, short-range structure and formation of iron phytate are studied with the help of two complementary spectroscopic techniques; X-ray absorption spectroscopy (EXAFS - Extended X-ray Absorption Fine Structure and XANES – X-ray Absorption Near Edge Structure) of iron K absorption edge and solid-state nuclear magnetic resonance (NMR) spectroscopy of ^{31}P nuclei. In addition to the elucidation of some structural properties of iron phytate, the contribution thus also demonstrates the useful methodological approach for the investigation of local atomic arrangement within an amorphous, paramagnetic iron-rich material.

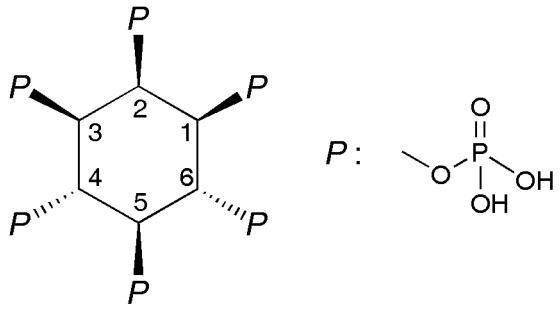

Scheme 1. Structure of *myo*-inositol hexaphosphoric acid.

Experimental section

All common laboratory chemicals were reagent grade, purchased from commercial sources and used without further purification. Ultrapure water obtained from a Millipore-MilliQ plus system was used throughout the work. An aqueous solution of phytate (Sigma) was prepared in 15 ml of 0.1M HNO_3. To prepare desired molar ratios, appropriate amounts of iron(III) ions were added to the above solution. Iron was added in a form of 0.25M $Fe(NO_3)_3 \times 9H_2O$ solution in 0.1M HNO_3. A white solid, which appeared immediately, was separated by centrifugation, washed with 0.1M HNO_3 (15 mL) and water (15 mL), and dried with ethanol (15 mL) and ether (15 mL).

Elemental analysis of solid samples was carried out by EDXS method on a scanning electron microscope Jeol JSM-5800 equipped with a LINK ISIS 300 system.

Magic-angle spinning ^{31}P NMR spectrum of iron phytate **1** was recorded on Varian Unity Inova 600 spectrometer, operating at ^{31}P Larmor frequency of 242.82 MHz, with rotation synchronized Hahn-echo pulse sequence. Sample rotation frequency was 20 kHz, repetition delay between consecutive scans was 0.1 s and number of scans was 40 000. Broadline ^{31}P NMR spectra of iron phytates **1** to **6** were recorded by the spin-echo mapping technique.[9,10] Schematically, the method consists of recording a series of spectra using Hahn echo sequence at different irradiation frequencies. For each spectrum the intensity was corrected taking into account the relaxation of the magnetization before acquisition of the signal. The total signal was obtained by addition of all individual spectra. All broadline NMR measurements were carried out on a Varian Unity Inova 300 spectrometer, operating at ^{31}P Larmor frequency of 122.65

MHz. The width of $\pi/2$ pulses was 2.5 μs and separation τ between the $\pi/2$ and π pulses was 25 μs. The irradiation frequency was incremented in 100 kHz steps and the number of increments was dictated by the frequency limits beyond which the NMR signal was negligible. In all spectra isotropic shift in ppm is reported relative to the signal of phosphorus nuclei within 85% solution of H_3PO_4. The decomposition of broadline ^{31}P NMR spectra was done by dmfit.[11]

X-ray absorption spectra in the energy region of the Fe K-edge were measured in transmission mode at E4 beamline of HASYLAB synchrotron facility at DESY in Hamburg and at ELETTRA XAFS (BL 11.1) beamline in Trieste. The E4 station provided a focused beam from an Au-coated torroidal mirror, with a focal spot of about 5mm x 1 mm on the sample. A Si(111) double crystal monochromator was used with about 1.5 eV resolution at the Fe K-edge (7112 eV). Harmonics were effectively eliminated by a plane Au-coated mirror, and by a slight detuning of the second monochromator crystal, keeping the intensity at 60 % of the rocking curve with the beam stabilization feedback control. The intensity of the monochromatic x-ray beam was measured by three consecutive ionization chambers filled with argon at a pressure of 80 mbar, 380 mbar and 680 mbar in the first, second and the third, respectively. At XAFS beamline of ELETTRA a Si(111) double crystal monochromator was used with about 0.8 eV resolution at the Fe K-edge. The three ionization chambers were filled with the following gas mixtures: first with 580 mbar N_2 and 1480 mbar He; second with 1000 mbar N_2, 90 mbar Ar and 910 mbar He; and third with 340 mbar Ar, 1000 mbar N2 and 660 mbar He.

The iron phytate samples were prepared as self-supporting pellets with absorption thickness (μd) of about 1 above the Fe K-edge. For comparison, the absorption spectra were measured also on the reference Fe samples with known valence state ($FeSO_4 \times 7\ H_2O$, $FePO_4 \times 2H_2O$, α-FeOOH, $Fe_2(SO_4)_3 \times 5H_2O$, $LiFePO_4$) For each reference sample micronised powder was homogeneously mixed with micronised BN powder and pressed in pellets with the total absorption thickness of about 1.5 above the Fe K-edge. The samples were mounted on a sample holder between the first and second ionization chamber. In the XANES region equidistant energy steps of 0.3 eV were used, while for the EXAFS region equidistant k-steps ($\Delta k \approx 0.03$ Å-1) or equidistant energy steps of 2 eV were adopted with an

integration time of 2s/step. Three repetitions were superimposed to improve signal-to-noise ratio. In all experiments the exact energy calibration was established with simultaneous absorption measurements on 5-micron thick Fe metal foil placed between the second and the third ionization chamber. Absolute energy reproducibility of the measured spectra was ±0.1 eV.

The relative K-shell contribution was obtained from the measured absorption spectra by a standard procedure[12]: i.e. by removing the extrapolated best-fit linear function determined in the pre-edge region (-250 .. -70 eV) and normalizing to a unit Fe K-edge jump. The zero energy was taken at the first inflection point in the Fe metal spectrum (7112 eV), i.e., at the 1s ionization threshold in the Fe metal. The quantitative analysis of EXAFS spectra was performed with the IFEFFIT program packages[13] using FEFF6 code[14] in which the photoelectron scattering paths were calculated ab initio from a presumed distribution of neighbor atoms.

Results and Discussion

Seven solid substances were prepared from a mixture of phytic acid and an increasing fraction of ferric ions. The substances were denoted with numbers **0.5**, **1**, **2**, **3**, **4**, **5**, and **6**, which reflect the number of moles of ferric ions added per one mole of phytic acid. The yield of the aggregated product depended on the concentration of iron within the initial mixture and was the smallest in case of preparation of substance **0.5**. This suggests that probably more than 0.5 moles of ferric ions per one mole of phytic acid were spent for formation of the solid product. The hypothesis is supported by the results of the EDXS elemental analysis of iron phytates, which are presented in Figure 1. Although the concentrations of ferric ions during preparation of substances **0.5**, **1**, and **2** were increasing successively, the resulting solids all contained approximately 2.5 iron ions per one molecule of phytate. It appears that roughly two or more ferric ions per one phytic molecule are needed for solid aggregates to be formed. Further increase of iron concentration within the initial mixture only slowly increases the fraction of iron within the aggregated solid, and it seems that the final fraction cannot exceed about four iron ions per one phytic molecule. This is expressed as a second plateau in Figure 1.

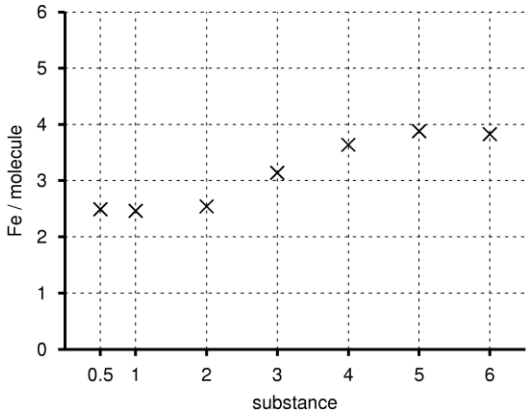

Figure 1. Results of EDXS elemental analysis of seven solid substances. Relative experimental error is smaller than 3%.

A more detailed and complementary picture of the formation of the solid iron phytate can be obtained by solid-state NMR investigation. Recently, we have witnessed a growing interest in solid-state NMR of paramagnetic compounds.[15-19] In such compounds, atomic nuclei are exposed to strong dipolar and hyperfine interactions with unpaired electrons from paramagnetic centres.[19] Strong orientation dependent interactions in powders can in principal lead to broad spectral lines and thus to reduced resolution of contributions from nuclei that occupy structurally inequivalent sites. However, recent examples show that very fast magic-angle sample spinning (MAS) can retrieve sufficient resolution in spectra of organic molecules with paramagnetic centres.[20,21] Furthermore, accelerated relaxation and enhanced isotropic shifts induced by the interaction with the nearby paramagnetic centers can actually speed up NMR measurements and aid in an assignment of spectral contributions and in structure solution of such materials.[22]

Because we expected iron ions to interact with phytate's phosphate groups, we were predominantly interested in ^{31}P NMR spectroscopy. However, phosphorus fast-MAS spectra of iron phytates (Figure 2) exhibit only one phosphorus contribution, which is split into a broad pattern of spinning sidebands. It appears that high-resolution spectra of phosphorus nuclei cannot be obtained in case of iron phytates. We encountered similar ^{31}P MAS NMR spectra for inorganic zeolite-like aluminophosphate materials, in which framework aluminum was partially substituted by nickel, cobalt, iron or manganese.[9] In these materials, bonding of a transition metal atom to a phosphorus atom, Me-O-P, induced isotropic shifts

that ranged from 1500 to 12000 ppm and extremely fast T_2 relaxation, which prevented MAS spectra to be detected. For the latter reason the phosphorus environment was in those materials studied by 'static' broadline NMR spectroscopy.

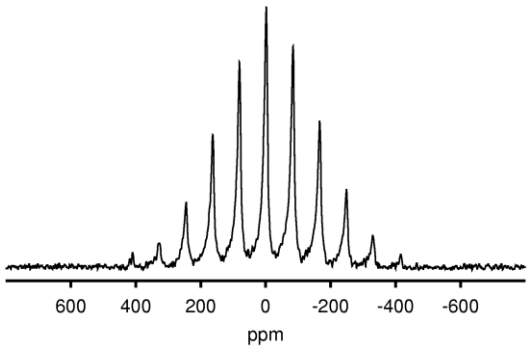

Figure 2. ^{31}P fast-MAS NMR spectrum of substance **1**.

Static ^{31}P NMR spectroscopy applied to substances **1** to **6** yields spectra, which are presented in Figure 3. The spectra are broad, extending over a region of more than 10000 ppm, and can in all cases be described by a sum of three contributions. Isotropic shifts of these three contributions are approximately 0, 4000 and 7000 ppm, and line widths (full width at half maximum) are about 570, 2900 and 5300 ppm, respectively. Position and width of the first contribution is typical for phosphorus within diamagnetic systems, thus it can be assigned to phosphorus nuclei that are not bonded to iron. Large isotropic shifts of the second and the third contribution are induced by a hyperfine interaction between ^{31}P nuclei and electron spins and are proportional to the isotropic hyperfine coupling constant A_{iso}.[19] A_{iso} is used to characterize magnetic coupling between two paramagnetic centers or between a paramagnetic center and a nucleus. In our case it is controlled by the nature and extent of the overlap between the iron, oxygen and phosphorus orbitals. It can be measured by ENDOR spectroscopy and also by NMR, where it is calculated from the isotropic shift. For phosphorus nuclei that contribute to the second peak with isotropic shift of about 4000 ppm, A_{iso} is approximately 5.3 MHz.[9] This value is close to the isotropic hyperfine coupling constant of 6 MHz, which was recently determined for ^{31}P nuclei in $FeAlPO_4$-20 by ENDOR spectroscopy.[23] The isotropic shift of 4000 ppm also matches the shift observed in ^{31}P NMR spectra of $FeAlPO_4$-34 and $FeAlPO_4$-36.[9] In all those $FeAlPO_4$ materials (numbers 20, 34 and 36 denote

different structural types) the amount of incorporated iron was sufficiently small that a phosphorus atom could be bonded to maximally one iron atom. Thus, the signal at 4000 ppm in ^{31}P NMR spectra of iron phytates can be assigned to phosphorus nuclei exhibiting one P-O-Fe bond, further referred to as P_{1Fe} nuclei. It should be emphasized that the large isotropic hyperfine-coupling constant proves an existence of P-O and Fe-O bonds with strong covalent character. Furthermore, this unequivocal detection of chemical bonds between iron and phosphorus also strongly supports the expectation that the aggregated solids are iron phytates.

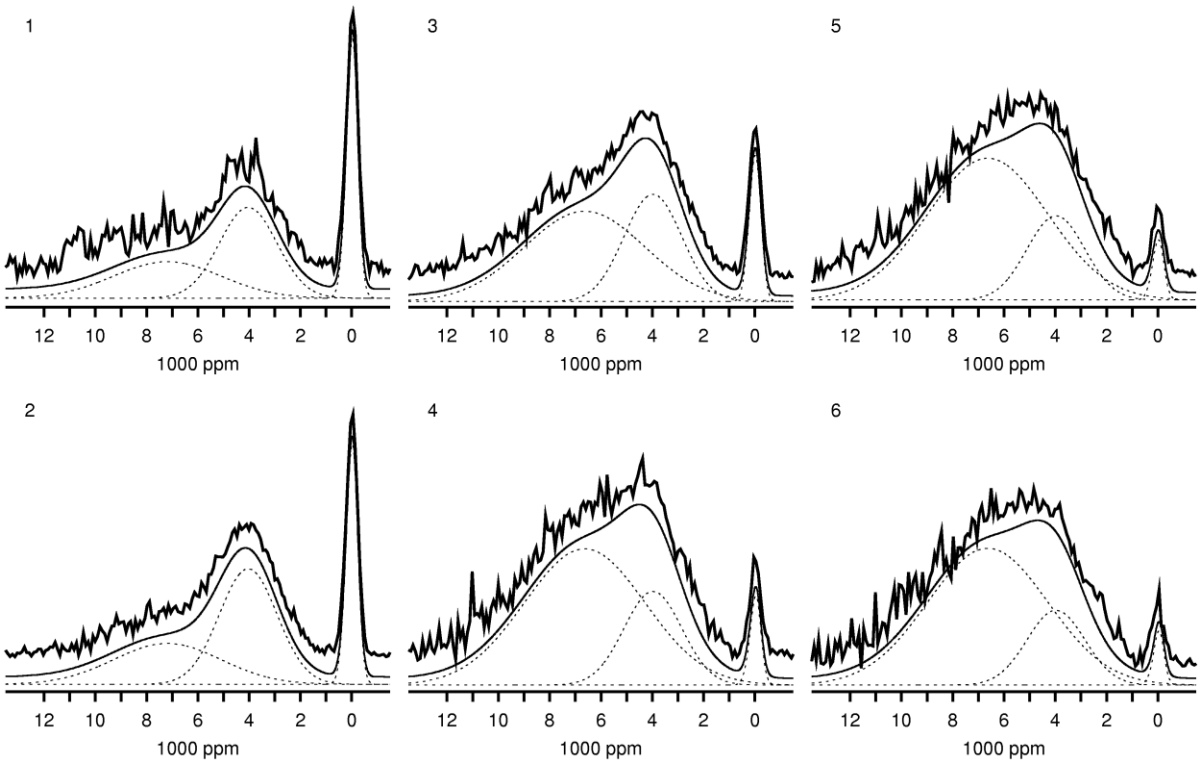

Figure 3. Broadline ^{31}P NMR spectra of substances **1** to **6**.

When paramagnetic centers within a material are sufficiently rare or when the temperature is sufficiently high that magnetic behavior of a material can be described by an ordinary Curie-Weiss law, effects of hyperfine couplings of several paramagnetic centers with one nucleus sum up and increase A_{iso}.[19] Recognizing that the isotropic shift of the broadest peak within ^{31}P spectra of iron phytates, 7000 ppm, corresponds to A_{iso} approximately twice as large as A_{iso} of P_{1Fe} nuclei, the widest contribution can be assigned to phosphorus nuclei with two P-O-Fe bonds. Let us denote these nuclei as P_{2Fe} nuclei. Thus, broadline ^{31}P NMR spectroscopy distinguishes among three different phosphorus environments

within iron phytates, P_{0Fe}, P_{1Fe} and P_{2Fe}, which differ by the number of P-O-Fe bonds that they exhibit. It should be stressed that in case of P_{2Fe} atoms we cannot determine if the two bonds are established with one or with two iron atoms.

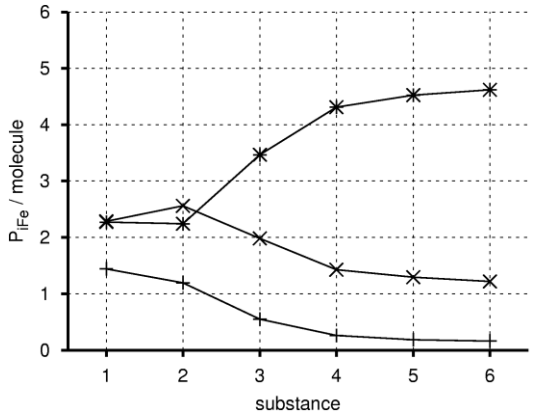

Figure 4. Average numbers of P_{0Fe} (+), P_{1Fe} (×) and P_{2Fe} (*) atoms per one phytic molecule determined from ^{31}P NMR spectra of iron phytates **1** to **6**.

Figure 4 shows average numbers of P_{0Fe}, P_{1Fe} and P_{2Fe} atoms per one phytic molecule, as determined from ^{31}P NMR spectra of iron phytates **1** to **6**. Note that each aggregated material can be a mixture of several 'domains', which are not equally rich in iron. Because the NMR analysis is performed on bulk samples, the obtained numbers of P_{0Fe}, P_{1Fe} and P_{2Fe} atoms per one phytic molecule reflect the average and are in general non-integer. Let us first consider these numbers of iron phytate **1**. Out of six phosphorus atoms of a phytic molecule, in average there are approximately 1.5 atoms not connected with iron. This suggests that at least four phosphorus atoms per one phytic molecule have to be bonded to iron in a solid iron phytate. Since we expect iron atoms to have a role of bridges between the adjacent phytic molecules, this assumption proposes that in solid iron phytate each phytic molecule could be connected to four neighboring phytic molecules. Such situation would resemble situations in many inorganic materials, where three-dimensional frameworks are formed by connecting tetrahedrally coordinated atoms to four nearby atoms via oxygen bridges. Studies of interaction between iron and inositol molecules, which have been conducted in solutions at minute addition of ferric ions, showed that iron interacts preferentially with phosphate groups in positions 1, 2 and 3 (see Scheme 1).[24,25]

However, the results described above indicate that interaction of ferric ions with only three phytic phosphate groups is not enough to induce aggregation of solid iron phytate.

As the fraction of iron within the initial mixture is increasing, the number of P_{2Fe} atoms is rising and the numbers of P_{0Fe} and P_{1Fe} atoms are dropping. In iron phytate **6**, the average number of P_{0Fe} atoms is only 0.2, which means that in the majority of the bulk sample all six phosphorus atoms of a phytic molecule are bonded to iron and one can say that phytate is almost saturated with iron. These observations match well to one of the hypothetical models for iron phytate structure proposed by Thompson and Erdman.[26] In this model each phosphorus is via oxygen bonded to two iron atoms and each iron atom is bonded to three phosphorus atoms and is shared between two phytic molecules (Scheme 2). The hypothetical structure would, however, be sterically very constrained and for phytic molecules it should be exceedingly difficult to arrange properly to allow this maximal iron concentration. The model thus only imposes an idealized limit to which one could asymptotically approach by increasing the concentration of iron within the initial mixture further and further. In our case, increasing initial concentration of ferric ions leads to aggregates, in which more and more but not all of the possible iron positions from the hypothetical model are occupied. Therefore the observed numbers of P_{2Fe} atoms are approaching the 'idealized' value of six and the numbers of P_{1Fe} and P_{0Fe} are tending to zero.

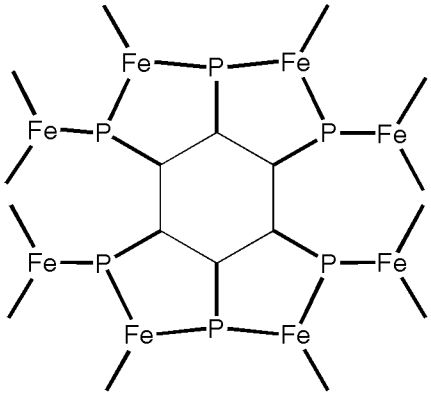

Scheme 2. Schematic representation of connections between phosphate groups and iron atoms in solid iron phytate according to the hypothetical model of Thompson and Erdman.[26] Oxygen bridges –O– are represented by thick lines while non-bridging oxygen atoms are omitted from the scheme for clarity.

The NMR results agree well with results of the elemental analysis. They all indicate that only such solid aggregates are formed, in which concentration of iron is sufficiently high that at least four phosphate groups of a phytic molecule can bond to iron and participate in the intermolecular connections. This lower limit in iron concentration is approximately two iron atoms per one phytic molecule. If iron concentration of the initial mixture is lower than that, all iron is used for aggregation of iron phytate whereas some phytic acid remains unreacted. The resulting solid thus still contains at least two iron atoms per one phytic molecule. That is why a plateau is observed for substances **0.5**, **1**, and **2** in Figure 1. When the initial concentration of iron exceeds two atoms per one phytic molecule, in average more than four phosphate groups of a phytic molecule bond to iron and form intermolecular bridges. However, there is also an upper limit in the concentration of iron, which is reached when all six phosphate groups of a phytic molecule bond to iron. According to the hypothetical model described above, the highest possible concentration of iron in solid iron phytate corresponds to four atoms per phytic molecule. The elemental analysis (Figure 1) shows that concentration of iron in substances **5** and **6** indeed approaches this value.

According to the discussion presented above a graph with two plateaus in Figure 1 can be explained by describing solid iron phytates as disordered networks of phytic molecules interconnected by iron bridges. For such a disordered network we can determine only an average number of connections between molecules, while the exact number of connections can in fact vary from one molecule in the network to another. However, the graph of Figure 1 could be obtained also if substances **1** to **6** were mixtures of two phases with two different and well-defined numbers of connections between molecules. One of the phases would be the major component of substance **1**, and the other one would be the major component of substance **6**. The average concentration of iron in samples **1** to **6** would then depend on two well-defined iron concentrations of the two phases and on the relative amounts of the two phases in the samples. It should be emphasized, however, that there is no experimental evidence indicating that the description with two well-defined phases is more appropriate than the description with disordered aggregates.

Combining NMR and elemental analyses offers additional information about bonding of iron with phosphate groups of phytic molecules. Namely, the NMR analysis provides the total number of P-O-Fe bonds per one phytic molecule, $N(P_{1Fe}) + N(P_{2Fe})$, and the elemental analysis provides the number of iron atoms per such a molecule. (Here $N(P_{1Fe})$ and $N(P_{2Fe})$ are numbers of P_{1Fe} and P_{2Fe} atoms per one phytic molecule, respectively.) By dividing the number of bonds with the number of atoms, one can obtain the average number of Fe-O-P bonds that an iron atom forms in solid iron phytates. Thus determined number of bonds using values from Figure 1 and Figure 4 is, within experimental precision, approximately 3 and it is equal for all substances **1** to **6** (Table 2). This indicates that iron in solid iron phytates preferentially establishes three bonds to the nearby phosphorus atoms. If the bonds were monodentate ones, the experimental indications about bonding of iron would again agree with the picture provided by the hypothetical model (see Scheme 2). However, the combination of NMR and elemental analyses cannot answer the question, whether bonds between phosphorus and iron are only monodentate ones or they are bidentate ones as well.

Additional insight into short-range structure of solid iron phytates can be obtained by examination of iron K-edge XANES and EXAFS spectra. The former offers information about the local symmetry and the valence state of iron, whereas the latter provides information about the local structure around iron atoms in the samples. The normalized Fe XANES spectra of iron phytate samples and reference compounds with known iron coordinations and oxidation states are shown in Figure 5. The shape of the K-edge and the pre-edge resonances are characteristic for the local symmetry of the investigated atom and can be used as fingerprints in identification of its local structure.[12,27-29] Tetrahedrally coordinated atoms, lacking an inversion center, exhibit a single pre-edge peak ($FePO_4$ in Figure 5), which can be assigned to 1s $\rightarrow$ 3d transition.[12,29,30] Octahedral symmetry is evident from two weak resonances in the pre-edge region assigned to transitions of 1s electron into antibonding orbitals with octahedral symmetry ($FeSO_4 \times 7H_2O$, $LiFePO_4$, $FePO_4 \times 2H_2O$ and $Fe_2(SO_4)_3 \times 5H_2O$ in Figure 5).[12,27-29] The XANES spectra of all iron phytate samples exhibit equal Fe K-edge profiles. The shape is characteristic for octahedrally coordinated iron and is almost identical as in the reference samples $FePO_4 \times 2H_2O$ and $Fe_2(SO_4)_3 \times 5H_2O$.

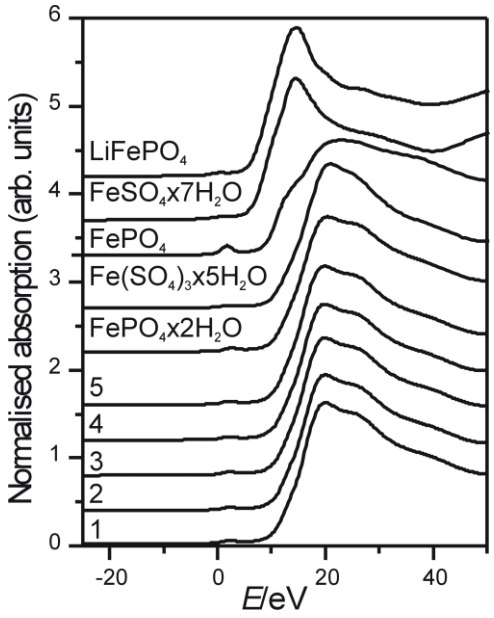

Figure 5. Normalized Fe K-edge XANES spectra of the iron phytate and reference iron compounds with known iron coordinations and oxidation states. The spectra are displaced vertically for clarity. The energy scale is relative to the Fe K-edge in Fe metal (7112 eV).

In addition, the Fe-K-edge shift can be used for determining the average valence state of iron in the sample. A linear relation between the edge shift and the valence state was established for atoms with the same type of ligands.[12,29] From the spectra of the reference samples ($FeSO_4 \times 7H_2O$, $LiFePO_4$, $FePO_4 \times 2H_2O$, α-FeOOH) with known iron oxidation states, we found that Fe K-edge shifts for 4 eV per valence state (Figure 5 and Figure 6), which is in agreement with previous observations.[31] Absorption derivatives of the Fe K-edge profiles from Figure 5 are plotted on Figure 6 to facilitate the comparison of edge shifts. The energy positions and the shape of the Fe K-edge of iron phytate samples is the same as in Fe(III) reference compounds $FePO_4 \times 2H_2O$ and $Fe_2(SO_4)_3 \times 5H_2O$, clearly indicating that iron valence state in all iron phytate samples is trivalent.

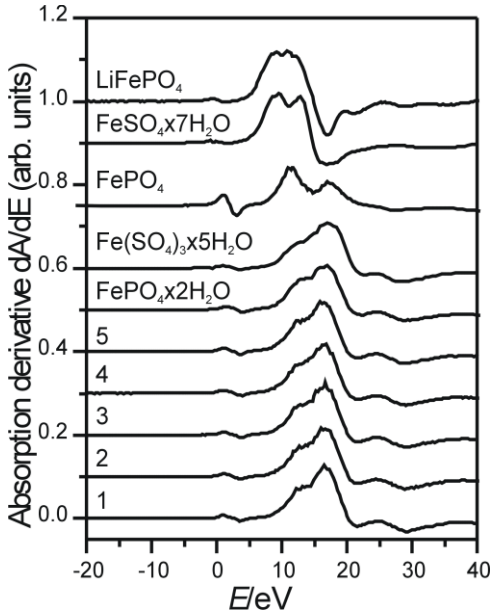

Figure 6. Absorption derivative of the Fe K-edge profile of the iron phytate and reference samples from Figure 5. The energy scale is relative to the Fe K-edge in Fe metal (7112 eV).

The Fe K-edge EXAFS spectra of the iron phytate samples (Figure 7) were quantitatively analyzed for the coordination numbers, distances, and Debye-Waller factors of the nearest coordination shells of iron. Fourier transform (FT) magnitudes of k^3-weighted Fe EXAFS spectra calculated in the k range of 4.5 - 14.5 $Å^{-1}$ are shown in Figure 7 together with best-fit EXAFS models. Two distinct peaks are found in all spectra. They represent the contributions of the first two shells of neighbors around iron atoms. From the comparison of the FT spectra some insight into the neighborhood of an iron atom can be obtained even before the detailed quantitative analysis is performed; first iron coordination shell is the same in all samples, the structural changes are indicated only in the second coordination shell by decreasing of the amplitude of the second peak with increasing amount of iron in the iron phytate sample.

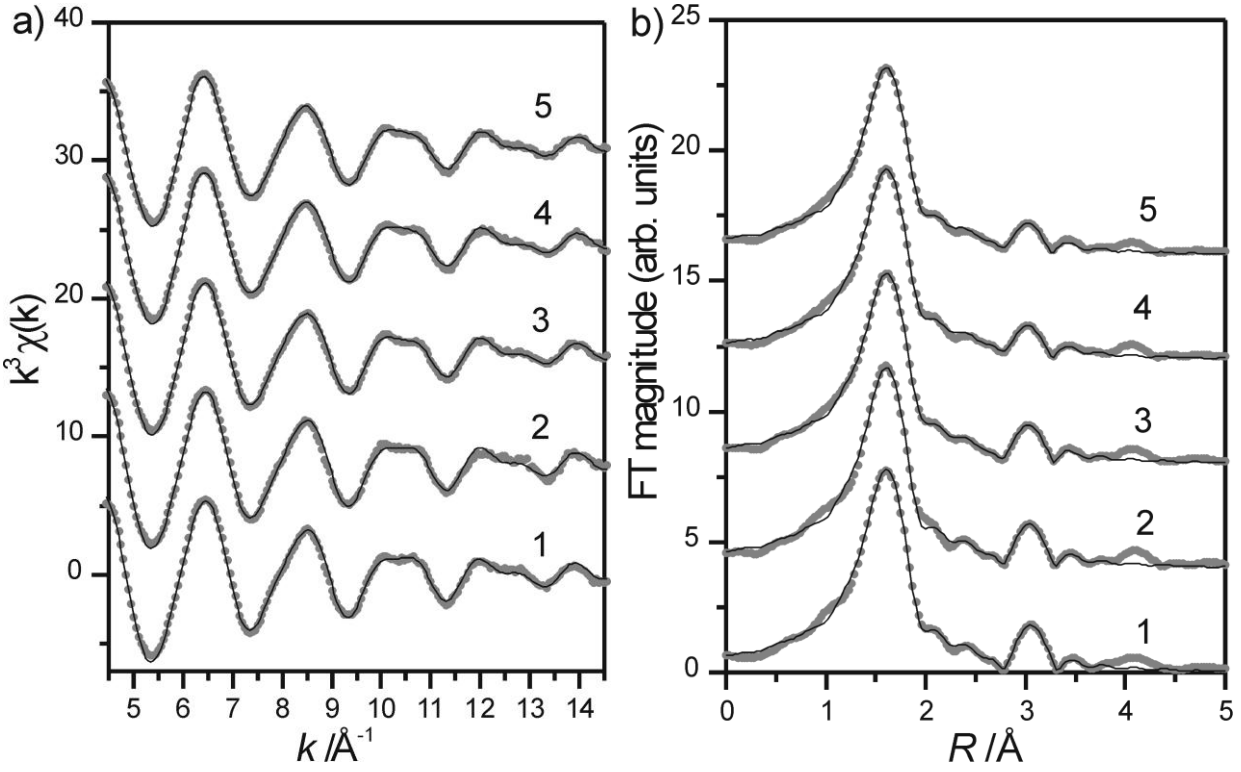

Figure 7. The k^3 weighted Fe EXAFS spectra of iron phytate samples (a) and corresponding Fourier transform magnitudes (b). In both parts dotted lines correspond to measured spectra and solid lines to best-fit EXAFS model.

The quantitative EXAFS analysis shows that the first iron coordination shell contains oxygen atoms, whereas the second shell consists of phosphorus and iron atoms. The atomic species of neighbors in consecutive shells were recognized by their specific scattering factors and phase shifts. The FEFF model, comprising all single scattering paths and all significant multiple scattering (MS) paths from the octahedral arrangement of oxygen atoms in the first coordination sphere (suggested by XANES spectra) and single scattering paths from a presumed distribution of iron and phosphorus atoms in the second coordination sphere, yields a very good fit in the k range of 4.5 Å^{-1} – 14.5 Å^{-1} and the R region from 1.1 Å to 3.6 Å (Figure 7). Contributions of individual scattering paths to the fit are shown in Figure 8 for the case of sample **1**. Three variable parameters were used for each shell of neighbors in the fit: the interatomic distance (R), the number of neighbors (N) at that distance and the corresponding Debye-Waller factor (σ^2). In case of MS paths from the octahedral arrangement of oxygen atoms in the first coordination sphere (24 triangular Fe-O-O (T) and linear Fe-O-O (L), Fe-O-Fe-O (L1 and L2) with

degeneracy 6) the path lenghts were constrained to the sum of coresponding single scattering distances within the octahedron. The Debye-Waller factor of the triangular MS paths is set to 1.5 times the value of σ^2 of the single scattering Fe-O paths, while for the linear MS paths a common Debye-Waller factor is varied in the fit. In addition, a common zero-energy shift ΔE_o was also varied. Complete list of best-fit parameters is given in Table 1. Relatively large uncertainties for the coordination numbers and Debye-Waller factors, especially for the shells of phosphorous atoms, are due to large correlations between fitting parameters N and σ^2 of these shells.

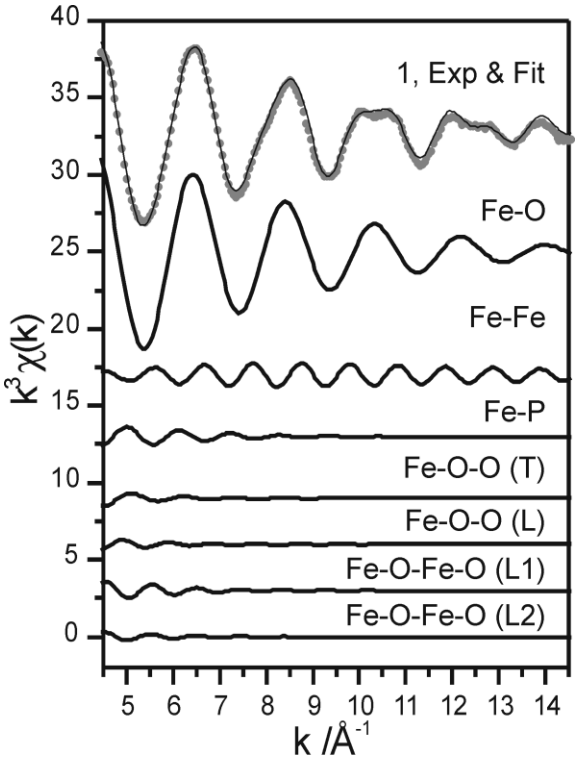

Figure 8. The k^3 weighted Fe EXAFS spectra of iron phytate sample **1** (dotted line) compared to the best-fit EXAFS model (solid line). Individual contributions from all single scattering paths (Fe-O, Fe-Fe, Fe-P) and multiple scattering paths from the octahedral arrangement of oxygen atoms in the first coordination sphere (triangular Fe-O-O (T) and linear Fe-O-O (L), Fe-O-Fe-O (L1 and L2)) included in the fit are shown below.

In all samples iron atoms are octahedrally coordinated to six oxygen atoms at 1.97 Å in the first coordination sphere. In the second coordination sphere three to four phosphorous atoms are identified at the distance of 3.32 Å. Together with results of ^{31}P NMR spectroscopy, which suggest that iron preferentially forms three bonds with phosphorus atoms, this implies that all Fe-O-P bonds are monodentate ones. The combination of EXAFS, NMR and elemental analyses thus finally elucidates that P_{2Fe} phosphorus atoms are bonded to two different iron atoms with monodentate bonds and not to one iron atom with a bidentate bond. Large Debye-Waller factor of the phosphorus shell indicates large static disorder in distribution of phosphorus atoms and is not surprising for amorphous substances. Additionally, in all samples approximately 0.5 iron atoms are identified at the distance of 3.35 Å, indicating that direct Fe-O-Fe bonds (in the form of linked FeO_6 octahedra, sharing one common oxygen atom) are present. The shape of EXAFS spectra rules out the possibility for the presence of nanosized iron-oxide impurities.[32] Average number of iron neighbors decreases from 0.6 in samples **1** and **2** to 0.45 in samples **4** and **5**. This means that only about half of iron atoms in solid iron phytates are directly linked by Fe-O-Fe bonds and that number of these bonds decreases with increasing amount of iron in the solid. The decrease is correlated with an increase in the number of phosphorus atoms within the second coordination shell and suggests that some Fe-O-Fe bonds are replaced by Fe-O-P bonds when concentration of iron in iron phytates is increased. An increase in the number of Fe-O-P bonds is accompanied by an increase in the number of P_{2Fe} atoms and a decrease in the numbers of P_{1Fe} and P_{0Fe} atoms. It should be stressed that although the uncertainty in the number of iron and especially phosphorus atoms in the second coordination shell is rather large, differences in these numbers are not negligible and they are clearly correlated with results of the elemental (Figure 1) and NMR analysis (Figure 4).

Finally, the observation, that significant number of Fe-O-Fe bonds exists in samples **1** and **2**, in which the total concentration of iron is substantially smaller than in sample **4** and **5**, is in line with the results of studies of interaction between iron and inositol-phosphate molecules in solution. These studies[24,25] show that iron interacts preferentially with phosphate groups in positions 1, 2 and 3. If in solid

aggregates the three groups are always bonded to iron atoms, then these atoms are sufficiently close one to another to form Fe-O-Fe bonds even in samples **1** and **2** and proximity among iron atoms in samples **4** and **5** is not necessarily larger. As already mentioned, the number of Fe-O-Fe bonds can actually decrease in the latter samples on account of the formation of additional P-O-Fe connections.

Conclusions

Broadline ^{31}P NMR and Fe K-edge X-ray absorption spectroscopy showed that bonds P–O–Fe with strong covalent character exist in solid iron phytates. Iron in these substances is trivalent, octahedrally coordinated by six oxygen atoms, and further monodentatly bonded to about three to four phosphorus atoms. In this way iron forms -P-O-Fe-O-P- bridges between the adjacent phytic molecules. In addition, approximately half of iron atoms are directly linked by Fe-O-Fe bonds. Iron phytates aggregate from a solution, if at least four out of six phosphate groups per one phytic molecule bond to iron. In this lower limit solid iron phytate contains at least two iron atoms per one molecule of phytate. The short-range structural properties of solid iron phytates with an increasing concentration of iron might well be explained by structures that are approaching an idealized model, in which each phosphate group is bonded to two iron atoms, and each iron atom is shared between two phytic molecules. Such a model contains four iron atoms per one molecule of phytate. Finally, broadline ^{31}P NMR and Fe K-edge X-ray absorption spectroscopy proved to be adequate techniques for the investigation of the short-range structure and of the bonding between individual molecules within amorphous iron phytates. They provided information, which had so far been unavailable by other experimental approaches.

Acknowledgment This work was supported by the Slovenian Research Agency research programme P1-0112 and J1-6350, by DESY, ELETTRA and the European Community under the FP6 Programme "Structuring the European Research Area" contract RII3-CT-2004-506008 (IA-SFS). Access to synchrotron radiation facilities of HASYLAB (beamline E4, project II-04-065) and ELETTRA

(beamline XAFS, project 2005156) is acknowledged. We would like to thank Edmund Welter of HASYLAB and Luca Olivi of ELETTRA for expert advice on beamline operation.

Figure Captions

Figure 1. Results of EDXS elemental analysis of seven solid substances. Relative experimental error is smaller than 3%.

Figure 2. ^{31}P fast-MAS NMR spectrum of substance **1**.

Figure 3. Broadline ^{31}P NMR spectra of substances **1** to **6**.

Figure 4. Average numbers of P_{0Fe} (+), P_{1Fe} (×) and P_{2Fe} (*) atoms per one phytic molecule determined from ^{31}P NMR spectra of iron phytates **1** to **6**.

Figure 5. Normalized Fe K-edge XANES spectra of the iron phytate and reference iron compounds with known iron coordinations and oxidation states. The spectra are displaced vertically for clarity. The energy scale is relative to the Fe K-edge in Fe metal (7112 eV).

Figure 6. Absorption derivative of the Fe K-edge profile of the iron phytate and reference samples from Figure 5. The energy scale is relative to the Fe K-edge in Fe metal (7112 eV).

Figure 7. The k^3 weighted Fe EXAFS spectra of iron phytate samples (a) and corresponding Fourier transform magnitudes (b). In both parts solid lines correspond to measured spectra and dotted lines to best-fit EXAFS model.

Figure 8. The k^3 weighted Fe EXAFS spectra of iron phytate sample **1** (dotted line) compared to the best-fit EXAFS model (solid line). Individual contributions from all single scattering paths (Fe-O, Fe-Fe, Fe-P) and multiple scattering paths from the octahedral arrangement of oxygen atoms in the first coordination sphere (triangular Fe-O-O (T) and linear Fe-O-O (L), Fe-O-Fe-O (L1 and L2)) included in the fit are shown below.

Scheme titles

Scheme 1. Structure of *myo*-inositol hexaphosphoric acid.

Scheme 2. Schematic representation of connections between phosphate groups and iron atoms in solid iron phytate according to the hypothetical model of Thompson and Erdman.[26] Oxygen bridges –O– are represented by thick lines while non-bridging oxygen atoms are omitted from the scheme for clarity.

Tables

Table 1: Quantitative results of EXAFS analysis, showing the composition of the nearest coordination shells around Fe atoms in iron phytate samples 1, 2, 3, 4 and 5. [a,b]

Substance	neighbors	*N*	*R* [Å]	σ^2 [Å^2]	*R*-factor
1	O	6.3 (3)	1.971 (5)	0.0076 (4)	0.002
	P	3 (1)	3.33 (2)	0.025(5)	
	Fe	0.6 (1)	3.35 (1)	0.003 (1)	
2	O	6.3 (3)	1.970 (5)	0.0075 (4)	0.003
	P	3 (1)	3.32 (2)	0.020 (5)	
	Fe	0.55 (5)	3.35 (1)	0.003 (1)	
3	O	6.1 (3)	1.974(2)	0.0078 (2)	0.0005
	P	4 (1)	3.31 (2)	0.023 (8)	
	Fe	0.50 (5)	3.34 (1)	0.003 (1)	
4	O	6.1(3)	1.972 (4)	0.0077 (4)	0.002
	P	4 (1)	3.30 (2)	0.020 (8)	
	Fe	0.46 (7)	3.34 (1)	0.003 (1)	
5	O	6.0 (3)	1.972 (3)	0.0078 (3)	0.002
	P	4 (1)	3.30 (2)	0.021 (8)	
	Fe	0.44 (7)	3.34 (1)	0.003 (1)	

[a]Average number of neighbor atoms (*N*), distance (*R*), Debye-Waller factor (σ^2), and the goodness-of-fit parameter, *R*-factor,[13] are listed. Uncertainty of the last digit is given in parentheses.

[b]A best fit is obtained with the amplitude reduction factor $S_0^2 = 0.85$, E_o shift of -0.9 (4) eV and the value of the Debye-Waller factor of linear MS paths of 0.02 (1) Å^2.

Table 2: Average number of Fe-O-P bonds formed by an iron atom in solid iron phytates as obtained from results of the elemental and NMR analysis. Relative experimental error is 15%.

1	**2**	**3**	**4**	**5**	**6**
2.8	2.8	2.9	2.8	2.7	2.7

References

(1) Zhou, J. R.; Erdman, J. W. *Crit. Rev. Food Sci. Nutr.* **1995**, *35*, 495.
(2) Frossard, E.; Bucher, M.; Machler, F.; Mozafar, A.; Hurrell, R. *J. Sci. Food Agric.* **2000**, *80*, 861.
(3) Shamsuddin, A. M.; Vucenik, I.; Cole, K. E. *Life Sci.* **1997**, *61*, 343.
(4) Daniels, V. D. *Chem. Soc. Rev.* **1996**, *25*, 179.
(5) Neevel, J. G. *Restaur.-Int. J. Preserv. Libr. Arch. Mater.* **1995**, *16*, 143.
(6) Kolar, J.; Strlič, M.; Novak, G.; Pihlar, B. *J. Pulp Pap. Sci.* **1998**, *24*, 89.
(7) Persson, H.; Turk, M.; Nyman, M.; Sandberg, A. S. *J. Agric. Food Chem.* **1998**, *46*, 3194.
(8) Torres, J.; Dominguez, S.; Cerda, M. F.; Obal, G.; Mederos, A.; Irvine, R. F.; Diaz, A.; Kremer, C. *J. Inorg. Biochem.* **2005**, *99*, 828.
(9) Mali, G.; Ristić, A.; Kaučič, V. *J. Phys. Chem. B* **2005**, *109*, 10711.
(10) Canesson, L.; Boudeville, Y.; Tuel, A. *J. Am. Chem. Soc.* **1997**, *119*, 10754.
(11) Massiot, D.; Fayon, F.; Capron, M.; King, I.; Le Calve, S.; Alonso, B.; Durand, J. O.; Bujoli, B.; Gan, Z. H.; Hoatson, G. *Magn. Reson. Chem.* **2002**, *40*, 70.
(12) Wong, J.; Lytle, F. W.; Messmer, R. P.; Maylotte, D. H. *Phys. Rev. B* **1984**, *30*, 5596.
(13) Ravel, B.; Newville, M. *J. Synchrotron Rad.* **2005**, *12*, 537.
(14) Rehr, J. J.; Albers, R. C.; Zabinsky, S. I. *Phys. Rev. Lett.* **1992**, *69*, 3397.
(15) Liu, K.; Ryan, D.; Nakanishi, K.; McDermott, A. *J. Am. Chem. Soc.* **1995**, *117*, 6897.
(16) Lee, H.; Polenova, T.; Beer, R. H.; McDermott, A. E. *J. Am. Chem. Soc.* **1999**, *121*, 6884.
(17) Ziessel, R.; Stroh, C.; Heise, H.; Kohler, F. H.; Turek, P.; Claiser, N.; Souhassou, M.; Lecomte, C. *J. Am. Chem. Soc.* **2004**, *126*, 12604.
(18) Sporer, C.; Heise, H.; Wurst, K.; Ruiz-Molina, D.; Kopacka, H.; Jaitner, P.; Kohler, F.; Novoa, J. J.; Veciana, J. *Chem.-Eur. J.* **2004**, *10*, 1355.
(19) Grey, C. P.; Dupre, N. *Chem. Rev.* **2004**, *104*, 4493.
(20) Ishii, Y.; Wickramasinghe, N. P.; Chimon, S. *J. Am. Chem. Soc.* **2003**, *125*, 3438.
(21) Wickramasinghe, N. P.; Shaibat, M.; Ishii, Y. *J. Am. Chem. Soc.* **2005**, *127*, 5796.
(22) Pintacuda, G.; Park, A. Y.; Keniry, M. A.; Dixon, N. E.; Otting, G. *J. Am. Chem. Soc.* **2006**, *128*, 3696.
(23) Arieli, D.; Delabie, A.; Vaughan, D. E. W.; Strohmaier, K. G.; Goldfarb, D. *J. Phys. Chem. B* **2002**, *106*, 7509.
(24) Spiers, I. D.; Barker, C. J.; Chung, S. K.; Chang, Y. T.; Freeman, S.; Gardiner, J. M.; Hirst, P. H.; Lambert, P. A.; Michell, R. H.; Poyner, D. R.; Schwalbe, C. H.; Smith, A. W.; Solomons, K. R. H. *Carbohydr. Res.* **1996**, *282*, 81.
(25) Phillippy, B. Q.; Graf, E. *Free Radic. Biol. Med.* **1997**, *22*, 939.
(26) Thompson, D. B.; Erdman, J. W. *Cereal Chem.* **1982**, *59*, 525.
(27) Heijboer, W. M.; Glatzel, P.; Sawant, K. R.; Lobo, R. F.; Bergmann, U.; Barrea, R. A.; Koningsberger, D. C.; Weckhuysen, B. M.; de Groot, F. M. F. *J. Phys. Chem. B* **2004**, *108*, 10002.
(28) Pantelouris, A.; Modrow, H.; Pantelouris, M.; Hormes, J.; Reinen, D. *Chem. Phys.* **2004**, *300*, 13.
(29) Arčon, I.; Mirtić, B.; Kodre, A. *J. Am. Ceram. Soc.* **1998**, *81*, 222.
(30) Bianconi, A.; Fritsch, E.; Calas, G.; Petiau, J. *Phys. Rev. B* **1985**, *32*, 4292.
(31) Benfatto, M.; Solera, J. A.; Ruiz, J. G.; Chaboy, J. *Chem. Phys.* **2002**, *282*, 441.
(32) Arčon, I.; Mozetič, M.; Kodre, A. *Vacuum* **2005**, *80*, 178.